

**ION TRANSFER ACROSS MEMBRANE STABILIZED LIQUID  
LIQUID INTERFACE.  
APPLICATION TO ENZYMATIC DETERMINATION OF UREA**

A Thesis

submitted to the

School of Graduate Studies

Addis Ababa University

In Partial Fulfillment of 

the Requirements for the Degree of

Master of Science in Chemistry

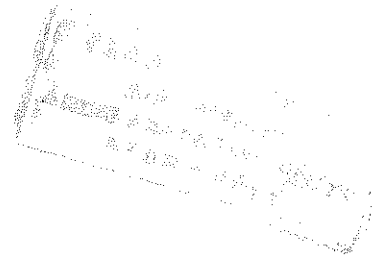
By

Sisay Tadesse

June 2000

## DEDICATION

To my wife Abaynesh Bekele and to my son Nathan Sisay.



## ACKNOWLEDGMENTS

First of all I would like to pay respect and express my indebtedness to my research advisor Dr Bernd Hundhammer whose untiring guidance in every phase of the research made it possible to materialize this work. I would like to express my deep appreciation for his interest in my work and generously gave his time, energy and valuable advice.

My heart-felt gratitude and appreciation goes to all my friends for their help, and encouragement at all stages of this research. Stimulating cooperation of the staff members of chemistry department (AAU) during my study at the university is gratefully appreciated.

Moreover, many thanks are attributed to all my colleagues in Awassa College of Teachers Education (ACTE) who helped me morally and materially to complete this work. My sincere appreciations also goes to Southern Nations Nationalities and Peoples Regional Government Education Bureau (SNNPRGEB) for giving me the opportunity to participate in the graduate programme.

My sincere thanks go to my wife W/o Abaynesh Bekele and my son Nathan Sisay for suffering without complaint, the brutishness to which I sink in order to do something they hope is worthwhile.

## TABLE OF CONTENTS

	Page
Acknowledgments.....	i
Table of contents.....	ii
List of figures .....	iv
List of tables.....	vi
Abstract.....	vii
1. Introduction.....	1
2. Literature review.....	4
3 Theory.....	9
3.1 Ion transfer.....	9
3.2 Non-polarizable ITIES and polarizable ITIES.....	13
3.3 Amperometric sensors based on charge transfer across liquid/liquid interfaces.....	15
3.4 Mathematical treatment of concentration profile at the membrane Stabilized interface.....	16
4. Experimental.....	22
5. Results and discussion.....	26
5.1 The influence of membrane on simple ion transfer.....	26
5.1.1 Cyclic voltammetry at membrane stabilized interface.....	27
5.1.2 Flow injection amperometry at membrane stabilized interface.....	28

5.1.3 Differential pulse voltammetry at membrane stabilized interface.....	32
5.1.4 Chronoamperometry, chronocoulometry and chronopotentiometry at membrane stabilized interface.....	33
5.2 The cyclic and differential pulse voltammetry study of facilitated transfer of ammonium ion with dibenzo-18-crown-6.....	40
5.3 The influence of employing single and double membrane on the facilitated transfer of ammonium ion.....	44
5.4 The response behavior of the urea sensor.....	47
6. Conclusion.....	51
7. References.....	52



## LIST OF FIGURES

	Page
Figure 1 Transfer of ions across water/oil interface.....	16
Figure 2 Distance concentration profile prior to application of a current step.....	17
Figure 3(a) Membrane stabilized structure of the enzyme sensor, and (b) The amperometric sensor.....	24
Figure 4 The four electrode potentiostat.....	24
Figure 5 Block diagram of electronic setup for dc cyclic voltammetry.....	25
Figure 6(a)Cyclic voltammogram and (b) the square root of sweep rate dependence on the peak current for the transfer of 1mM ClO <sub>4</sub> <sup>-</sup> (Water→nitrobenzene).....	27
Figure 7 Dependence of peak current on the applied potential difference.....	32
Figure 8 Differential pulse voltammetry of 10 <sup>-3</sup> M NO <sub>3</sub> <sup>-</sup> and 3X10 <sup>-4</sup> M Cs <sup>+</sup> .....	33
Figure 9(a) Experimental chronoamperometric response of the membrane stabilized interface ITIES to a potential step excitation(current as a function of time)(b) Experimental chronoamperometric response of the membrane stabilized interface ITIES to a potential step excitation (Current as a function of inverse squareroot of time).....	36
Figure 10 Experimental chronocoulometric response of the membrane stabilized ITIES to a potential step excitation( current as a function of square root of time).....	37
Figure 11 Experimental chronopotentiometric response of the membrane stabilized ITIES to a current-step excitation.....	38

Figure 12 Inverse of current step dependence on the square root of transition time of the membrane stabilized ITIES.....	39
Figure 13. Plot of transition time constant $i\tau^{1/2}$ versus $i$ .....	40
Figure 14 Dibenzo-18-crown-6.....	41
Figure 15(A) square root of sweep rate dependence on the peak current, (B) cyclic voltammogram of $2 \times 10^{-4} \text{M NH}_4^+$ at sweep rates of 50, 25, 10 and 5 mV/s for 1, 2, 3 and 4 respectively.....	42
Figure 16 Differential pulse voltammetry of $2 \times 10^{-5} \text{M NH}_4\text{NO}_3$ .....	43
Figure 17 Potential excitation wave form for DPTB.....	44
Figure 18 Pulsed amperometric response to (A) single membrane and (B) double membrane .....	45
Figure 19 Pulse amperometric response after incorporating gelatin between two membranes.....	46
Figure 20(A) Cyclic voltammograms of the membrane stabilized water/nitrobenzene interface at increasing concentration of $\text{NH}_4^+$ (B) The concentration dependence on peak current at sweep rate of 25 mV/s.....	48
Figure 21 (a) pulse amperometric sensor response to concentration steps of 0.02 mM $\text{NH}_4^+$ , (b) Calibration curve for $\text{NH}_4^+$ ion obtained by pulsed amperometry.....	49
Figure 22(a) Pulse amperometric response to concentration steps of 0.08 mM, for 1 and 0.16 mM for 2, 3 and 4 of urea respectively.....	50

## LIST OF TABLES

	Page
Table 1 The measured thickness of different membranes.....	26
Table 2 Diffusion coefficient of $\text{ClO}_4^-$ evaluated from peak current versus square root of sweep rate and from convoluted cyclic voltammogram.....	28
Table 3 Results flow injection amperometric experiment.....	30
Table 4 Results of chronoamperometry at different potential steps for $10^{-6}\text{mol.cm}^{-3}$ $\text{LiNO}_3$ .....	35
Table 5 Results of chronocoulometry at different potential steps for $10^{-6}\text{mol.cm}^{-3}$ $\text{LiNO}_3$ .....	35
Table 6 Data extracted from Figure 12.....	39



## ABSTRACT

Ion transfer across the membrane-stabilized water/nitrobenzene interface has been investigated. The response behavior of the sensor has been studied employing different hydrophilic dialysis membranes and membrane filters. The influence of the membrane on the transfer of different cations and anions was investigated. Theoretical equations have been obtained for current step excitation and were compared with experimental results. The influence of supporting electrolyte concentration in the aqueous phase has been also investigated and it was observed that as the concentration of supporting electrolyte increases the diffusion through the membrane became faster.

The diffusion coefficients evaluated by employing different membrane materials were in the order of  $10^{-6}$  and  $10^{-7}$   $\text{cm}^2/\text{s}$ . The results obtained indicate higher diffusion coefficients for cations over anions.

The enzymatic amperometric sensor with immobilized urease enzyme based on the membrane stabilized interface was employed for the determination of urea. The facilitated transfer of ammonium ion has been formed in the enzymatic decomposition of urea and has been utilized for the determination of urea. The impact of membrane material employed and the incorporation of gelatin was investigated. The current response of the sensor was measured by pulse amperometry. The time constant of the urea sensor has been determined to be 250s.

## 1. INTRODUCTION

Since the development of enzyme-based amperometric sensor for glucose by Clark [1] in 1962 a wide variety of amperometric sensors has been described. They are based on the enzymatic conversion of the analyte into a form that can be conveniently detected electrochemically. Amperometric sensors were thus restricted to products which can either be oxidized or reduced at a suitable electrode material.

Over the years, there has been a steady growth in the use of enzymes as analytical tools in the industrial, medical pharmaceutical, and food fields. Among the enzymes that have been used in analytical systems, urease is one of the best known and extensively studied [2,3].

For many reasons, enzymes were being used on increasing scale. Characterized as being both specific and sensitive, yet easy to use and reproducible, enzymes were shown to be rather unique but powerful catalysts. However there were serious limitations to their use on any regular basis. They had very limited stability in aqueous solution with a consequent loss of catalytic activity. This was changed with the introduction of immobilized enzymes [4-6]. Free or water-soluble enzymes were immobilized or made insoluble by combination with some inert matrix either by entrapment or chemical reaction to ensure insolubility. In either case it was shown that enzymes retained activity for long periods of time. Thus it has been noted that a single sample of immobilized glucose oxidase has been used for several thousand

determinations [4].

Enzyme electrodes have probably been the most interesting application of immobilized enzymes. These electrodes have been the combination of an insoluble enzyme with some porous organic polymer which is used as a coating for electrochemical sensor.

Utilizing the current due to ion transfer across the interface of two immiscible electrolyte solutions offers an alternative amperometric method for the determination of a reaction products which can neither be oxidized or reduced. The stabilization of the liquid/liquid interface by a hydrophilic membrane is a necessary requirement to construct practicable amperometric sensors for ions the transfer of which can be studied [15]. The performance of these sensors is strongly influenced by the properties of the membrane material employed in constructing the sensor. Systematic investigations on the influence of the membrane material was carried out in this project.

The enzymatic sensor employed for the determination of urea was based on the membrane stabilized interface the enzyme sandwiched between two dialysis membranes and was based on the facilitated transfer of ammonium ion formed in the enzymatic hydrolysis of urea. In this method, the current due to the facilitated transfer of ammonium ion from aqueous to an organic phase is proportional to the ion concentration. Urea is hydrolyzed by the enzyme urease and the optimum pH for the activity of this enzyme has been reported to range from 6.5 to 9. [8]

The objective of the present research is to investigate the influence of the membrane and gelatin layers on the response behavior of the amperometric sensor, to develop an amperometric sensor for urea based on immobilized urease at the sensor surface and to check the applicability of the sensor for the determination of urea.



## 2. LITERATURE REVIEW

Urea is the dominant nitrogen fertilizer in world agriculture. Consumption is estimated to be thirty million metric tons annually. Hence special attention should be given to problems encountered with the use of urea as a fertilizer. These problems result largely from the rapid enzymatic hydrolysis of urea to ammonia and carbon dioxide [7].

There are several methods for the determination of ammonium ion that may be generated by the decomposition of urea [7,62,63]. The standard method used for the determination of ammonium in soils is the kjeldahl distillation method [63].

Electrochemical studies on ion transfer across the polarized water/oil interface have shown that this interface can be employed for voltammetric and amperometric determination of ions as an alternative to the common potentiometric method[64-67]. Amperometric method has the principal advantage that the electrical current signal is directly proportional to the concentration, and that the selectivity of the detector can be varied by means of a change in the electrode potential.

Guilbault and montalvo [9] constructed the first urea sensor by immobilizing urease on a glass ammonium-selective electrode. The electrode had an enhanced sensitivity to other ions like potassium and sodium. Later on, they constructed three types of electrodes [10]. The first one was made by covering the glass electrode with acrylamide gel-immobilized urease. The second one was made by adding cellophane

films over the enzyme layer and for the third type, the enzyme gel was sandwiched between two cellophane films. The presence of cellophane films had little effect on the response time of the sensor, but its stability was prolonged owing to the prevention of the leaching out of urease by the cellophane film. In order to increase the sensitivity Guilbault and Harbankova [11] added ion-exchanger resins to their samples and later, Guilbault and Nagy [12] used nonactin based ammonium ion selective electrode in which the nonactin was embedded in a silicone rubber matrix.

The application of an amperometric sensor for ammonium ion has been reported by Senda and Yamamoto [13]. Urease was immobilized on the sensor and the facilitated ammonium ion transfer from aqueous to nitrobenzene, in which the organic phase contained dibenzo-18-crown-6 and tetrabutylammonium tetraphenylborate as supporting electrolyte, was monitored. The current response of the sensor was measured by pulse amperometry.

Stabilization of liquid/liquid interfaces by insertion of porous membrane (either hydrophilic or lipophilic) has been successfully used to construct liquid state ion-selective electrodes (ISEs) [14], to investigate interfacial reactions [15] and to study ion transfer reaction at liquid/liquid interfaces [15,16]. The membrane-stabilized liquid/liquid interface has also been utilized as an amperometric sensor for the analytical determination of anions [17] and the simultaneous determination of  $\text{Na}^+$  and  $\text{K}^+$  in drinking water and foods using DB-15-C-5 as a neutral carrier in nitrobenzene [17]. Electrochemical investigations of ion transfer across these interfaces have yielded

additional information about membrane diffusion coefficients [15].

These ion transfer reactions can serve as the simplest model for the charge transfer reactions taking place in the living cells. In order to get a better picture of the biological original, the liquid/liquid interface can be modified in different ways [18,19]. Separation of two phases by a porous membrane may be one possibility in approaching this aim. Alberty et al. [20,21] have shown that the kinetics of systems reacting at the interface between two liquid phases can be studied successfully if the interface is established by surface tension on the pores of a millipore filter. If a hydrophilic membrane is used between the two phases, the space occupied by the membrane will exhibit different properties with respect to the aqueous phase. These differences can be reflected in the cyclic voltammograms obtained with and without a membrane and they will be caused, for example by changes of the diffusion coefficient within the membrane or by ion exchange if the membrane material exhibits ion exchange properties. On the other hand there is another possibility of altering the properties of the membrane by chemical modification either at the aqueous or at the organic side of the membrane. Chemical modification of the membrane could be used as a method to build up structures similar to biological membranes [22].

The transfer of alkali metal and alkaline earth metal ions across the organic solvent or oil(o) / water(w) interface facilitated by the presence of natural or synthetic ionophores, such as valinomycin, nonactin and crown ethers in the organic phase, has been intensively studied by Koryta [23] and his group,[24-31]. Despite the great effort

devoted to elucidate the mechanism of the ionophore-mediated ion transport, the central question about the site of the complex formation and its dissociation, whether it is in the organic phase, in the aqueous phase or at the interface, has not been settled yet. Koryta et al. [28] came into the conclusion that the valinomycin-facilitated transfer of potassium ion across the nitrobenzene/water interface takes place via two mechanisms, in the organic and at the interface in parallel. Experimental results suggesting the interface reaction mechanism have also been presented [34]. By contrast Yoshida and Freiser [33] have presented experimental evidence which they interpret as meaning that potassium ion reacts in the aqueous phase with valinomycin that has transferred from nitrobenzene phase. Lin and Freiser [35] have presented further experimental results suggesting that the mechanism of the potassium ion transfer facilitated by dibenzo-18-crown-6 across the 1,2-dichloroethane /water interface may depend on the concentration of potassium ion in the aqueous phase. The facilitated transfer of the alkali metal ions at the o/w interface is a very rapid process and is diffusion controlled when observed using electrochemical methods such as cyclic voltammetry, [23-31,34] chronopotentiometry, [32] and current-scan polarography with an electrolyte dropping electrode [33]. Kakutani et al. [36] stated that, the ac polarographic behavior of the transfer of  $\text{Na}^+$  ion facilitated by DB-18-C-6 at the nitrobenzene/ water interface is explained most reasonably by the interface reaction mechanism of the three mechanisms that have been proposed.

Ion transfer across the interface of immiscible electrolyte solutions has been studied extensively during recent years employing different organic phases and by different



electrochemical techniques [37-39]. When the crystal violet tetrapheylborate (CVTPB) is utilized as the supporting electrolyte in the organic phase and  $\text{Li}_2\text{SO}_4$  or  $\text{LiF}$  in the aqueous phase, the investigation of the transfer of relatively hydrophilic anions, such as  $\text{SCN}^-$ ,  $\text{I}^-$ , and  $\text{NO}_3^-$ , becomes possible [40-42].

One of the problems with studies at the ITIES is the high uncompensated Ohmic resistance usually encountered in practice. For the accurate determination of kinetic parameters, IR compensation techniques can be used conveniently. However, when compensation values greater than  $1000\Omega$  have to be used for potentiostatic measurement, the systems are often prone to oscillations. Furthermore the potentiostatic experiments with ascending electrolyte drops, overcompensation can easily occur. To avoid these problems, Kihara used current-scan technique in which the correction for the uncompensated cell resistance was accomplished directly by subtracting from the measured potential the IR drop across a resistance in series with the galvanostat [43]. Z. Samec et al [44] showed that Ohmic drop in the solution can be compensated automatically by means of positive feedback loop, which is often used for the elimination of the Ohmic drop in the voltammetric measurements with three electrode systems.[45]

### 3. THEORY

#### 3.1. ION TRANSFER

At the liquid/liquid interface ion transfer can be classified in to simple and facilitated ion transfer which can be facilitated by complexation, ion pair formation and precipitation.

For a simple ion transfer across interface between two immiscible electrolyte solutions (ITIES) of the type,



at equilibrium the electrochemical potentials of the ion in both phases are equal

$$\bar{\mu}(\alpha) = \bar{\mu}(\beta) \quad (2)$$

or

$$\mu^0_i(\beta) + \frac{RT}{zF} \ln a_i(\beta) + zF\phi(\beta) = \mu^0_i(\alpha) + \frac{RT}{zF} \ln a_i(\alpha) + zF\phi(\alpha) \quad (3)$$

and for a reversible diffusion controlled ion transfer the Galvanipotential difference formed at the interface is given by

$$\Delta^{\alpha}_{\beta} \phi_i = \Delta^{\alpha}_{\beta} \phi_i^0 + \frac{RT}{z_i F} \ln \frac{a_i(\beta)}{a_i(\alpha)} \quad (4)$$

Since  $a = \gamma C$

$$\Delta^{\alpha}_{\beta} \phi_i = \Delta^{\alpha}_{\beta} \phi_i^0 + \frac{RT}{z_i F} \ln \frac{\gamma_i(\beta)}{\gamma_i(\alpha)} + \frac{RT}{z_i F} \ln \frac{C_i(\beta)}{C_i(\alpha)} \quad (5)$$

where  $a_i$ 's are the ion activities in the respective phases,  $\phi$ 's are the Galvani potentials of the individual phases, the  $\mu_i^0$ 's are standard chemical potentials and  $\gamma_i$  is the activity coefficient of the ion  $i$ . The  $\mu_i^0$ 's are quantities which are not accessible to direct measurement. At the interface a Galvanipotential difference,  $\Delta_{\beta}^{\alpha}\phi$ , is formed where

$$\Delta_{\beta}^{\alpha}\phi = \phi(\alpha) - \phi(\beta) \quad (6)$$

From equation 5, this is equal to

$$\Delta_{\beta}^{\alpha}\phi = \frac{\mu_i^0(\beta) - \mu_i^0(\alpha)}{z_i F} + \frac{RT}{z_i F} \ln \frac{a_i(\beta)}{a_i(\alpha)} \quad (7)$$

or

$$\Delta_{\beta}^{\alpha}\phi_i = \Delta_{\beta}^{\alpha}\phi_i^0 + \frac{RT}{z_i F} \ln \frac{a_i(\beta)}{a_i(\alpha)} \quad (8)$$

Where  $\Delta_{\beta}^{\alpha}\phi_i^0$  is the standard Galvanipotential difference.

The standard Gibbs energy of transfer of the cation  $i$  from the phase  $\alpha$  to phase  $\beta$ ,  $\Delta G_{tr}^{\alpha-\beta}$  is defined by

$$\Delta G_{tr}^{\alpha-\beta}, i = \mu_i^0(\alpha) - \mu_i^0(\beta) \quad (9)$$

This quantity is the difference of standard Gibbs energies of solvation of cation  $i$  in phase  $\alpha$  and phase  $\beta$  respectively. Thus

$$\Delta_{\beta}^{\alpha}\phi = \frac{\Delta G_{tr,i}^{0\alpha-\beta}}{z_i F} + \frac{RT}{z_i F} \ln \frac{a_i(\beta)}{a_i(\alpha)} \quad (10)$$

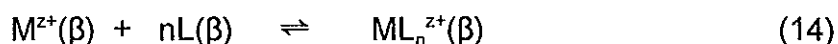
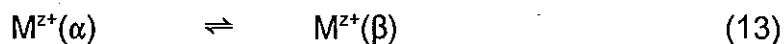
The flux balance at the half-wave potential is given by

$$(D^{1/2}_i(\alpha)C_i(\alpha))_{x=0} = (D^{1/2}_i(\beta)C_i(\beta))_{x=0} \quad (11)$$

Since equation 10 is the same as equation 4, combining with equation 11 the half wave potential is given by

$$\Delta^{\alpha}_{\beta}\phi_{1/2,i} = \Delta^{\alpha}_{\beta}\phi_i^0 + \frac{RT}{z_i F} \ln \frac{Y_i(\beta)}{Y_i(\alpha)} + \frac{RT}{2z_i F} \ln \frac{D_i(\alpha)}{D_i(\beta)} \quad (12)$$

The presence of specific ion complexes in one of the two phases is expected to result in significant shifts in the value of transfer potential. Let us consider the following reaction scheme.



The Nernst equation for the diffusion-controlled process is valid. And the concentration of the free metal ion  $M^{z+}$  in phase  $\beta$  must be expressed by using the equation for the stability constant of the complex formed:

$$[M^{z+}](\beta) = \frac{[ML_n^{z+}](\beta)}{K_{st}[L]^n(\beta)} \quad (15)$$

Where  $[M^{z+}](\beta)$  is the metal ion concentration,  $[L](\beta)$  the concentration of specific ion ligand,  $[ML_n^{z+}](\beta)$  the concentration of the complex,  $_{st}K$  represents the stability constant of the complex. Since charge transfer reactions across the ITIES are in general reversible, the Galvani potential difference between the phases  $\alpha$  and  $\beta$  is given by

$$\Delta_{\beta}^{\alpha} \phi_i = \Delta_{\beta}^{\alpha} \phi_{M^z}^0 + \frac{RT}{zF} \ln \frac{a_M^{z+}(\beta)}{a_M^{z+}(\alpha)} \quad (16)$$

$$= \Delta_{\beta}^{\alpha} \phi_{ML_n^z}^0 + \frac{RT}{zF} \ln \frac{a_{ML_n^z}^{z+}(\beta)}{a_{ML_n^z}^{z+}(\alpha)} \quad (17)$$

Considering the simplified equilibria of scheme 13 and 14 the Galvani potential difference for this system is

$$\Delta_{\beta}^{\alpha} \phi_{M^z} = \Delta_{\beta}^{\alpha} \phi_{M^z}^0 + \frac{RT}{zF} \ln \frac{a(\beta)_{M^z}}{a(\alpha)_{M^z}} \quad (18)$$

$$= \Delta_{\beta}^{\alpha} \phi_{M^z}^0 + \frac{RT}{zF} \ln \frac{C_{ML^z}(\beta)}{K_{st} C_L(\beta)^n C_{M^z}(\alpha)} \quad (19)$$

where  $\Delta_{\beta}^{\alpha} \phi_{M^z}^0$  is the formal potential for ion transfer which includes the activity coefficient terms. Since  $C_{M^z}(\alpha)$  is in excess, only the diffusion of L and  $ML_n^{z+}$  in phase  $\beta$  need to be considered. At the half wave potential the following condition applies:

$$(D_{ML_n^z}(\beta))^{1/2} (C_{ML_n^z}(\beta))_{x=0} = (D_L(\beta))^{1/2} (C_L(\beta)^n)_{x=0} \quad (20)$$

The half wave potential is given by

$$\Delta_{\beta}^{\alpha} \phi_{1/2, ML_n^z} = \Delta_{\beta}^{\alpha} \phi_{M^z}^0 + \frac{RT}{2zF} \ln \frac{D_L}{D_{ML_n^z}} - \frac{RT}{zF} \ln K_{st} C_{M^z}(\alpha) \quad (21)$$

From equation 21 it can be seen that the stability constant  $K_{st}$  can be calculated from ion transfer experiments assuming the diffusion coefficient of the ligand is the same as that of the complex. Further more, from cyclic voltammetry experiments it can be seen

that this type of facilitated ion transfer is completely diffusionally controlled, as the peak current depends linearly on the square root of the sweep rate and the ionophore concentration. Therefore, it can be used for the electroanalytical determination of ions (or conversely ionophores), which normally would transfer completely outside the potential window. As the size of the complex is approximately determined by the size of the ligand, it holds that  $D_L(\beta) \approx D_{MLnz^+}(\beta)$ . Thus we have

$$\Delta_{\beta}^{\alpha} \Phi_{1/2, ML_n^z} = \Delta_{\beta}^{\alpha} \Phi^0 - \frac{RT}{zF} \ln K_{st} C_{M^z}(\alpha) \quad (22)$$

In view of equation 21, stronger complexation and higher concentration of the metal ion cause larger shift of the half wave potential ( and, in the same way the peak potential) to more negative potential.

### 3.2 NON-POLARIZABLE ITIES AND POLARIZABLE ITIES

The fundamental difference between the two cases is that a non-polarizable interface refers only to an electrostatic equilibrium where the constituents of each phase have an infinite standard Gibbs energy of transfer, whereas a polarizable interface always refers to a chemical equilibrium. In the first case, when a potential difference is applied, no current flows across the interface. On the other hand, in the second case, when a potential is applied, electrical current must flow to establish the chemical equilibrium. Consequently, if this current is small enough to be considered negligible, the interface will be called polarizable. The definition of polarizability therefore implies the definition

of a current threshold level under which a current is considered negligible, and the region for which this condition applies is called the polarization window. [43]

In practice, ITIES can be polarized if the aqueous electrolyte is very hydrophilic and the organic salt very hydrophobic.

The ITIES for example water (w) and an organic liquid (o) as solvents, has several basic features analogous to the interface metallic electrode/electrolyte solution [23]. Between both liquid phases there is established electric potential difference which in cases where both phases contain a common ion I a charge number z follows the Nernst Donnan equation.

$$\Delta^w_{\circ}\phi_I = \Delta^w_{\circ}\phi_i^0 + \frac{RT}{z_i F} \ln \frac{a_i(o)}{a_i(w)} \quad (23)$$

Where  $\Delta\phi$ 's are the Galvani potential difference, and  $a_i$ 's activities of the ion I in each phase. These activities are defined, for example on molar scale; in the case of limiting dilution they approach molar concentration. The quantity  $\Delta G_{tr}^{o \rightarrow w}$  is the standard Gibbs energy of transfer from the organic to the aqueous phase for the ion I. In order to attribute a definite value to this quantity an extra thermodynamic approach has to be used, for example, the "Tetraphenylarsonium tetraphenylborate (TPATPB) assumption" stating that the standard transfer Gibbs energies of tetraphenylarsonium cation and of tetraphenylborate anion are equal for any pair of solvents [46]. On the basis of this assumption, scales of standard Gibbs transfer energies and of standard electrical



potential differences  $\Delta\phi$ ,  $\phi$  can be composed [47,48]. If there are semihydrophobic ions present in the system at a low concentration, the introduction of a charge to a phase can cause their transfer to occur in the potential window. Thus they can give an effect analogous to those shown by electroactive species in methods like voltammetry or chronopotentiometry.[49]

The potential difference  $\Delta\phi$  is defined by

$$\Delta\phi = \phi(w) - \phi(o) \quad (24)$$

so that the electrical potential of the organic phase  $\phi(o)$  is subtracted from the potential of the aqueous phase  $\phi(w)$ . The flow of positive charge from the aqueous to the organic phase corresponds to positive electrical current [50].

### 3.3 AMPEROMETRIC SENSORS BASED ON CHARGE TRANSFER ACROSS LIQUID/LIQUID INTERFACES

Ions can be transferred across a water/oil interface when an appropriate potential difference is applied. The current  $i$  due to the ion transfer is proportional to the concentration of the ion and can be utilized for the quantitative determination of ions.[51]

$$i = \sum k_j \cdot C_j \quad (25)$$

The partial sensitivity  $k_j$  is a function of the applied potential. Thus by varying the potential various ions can be determined.



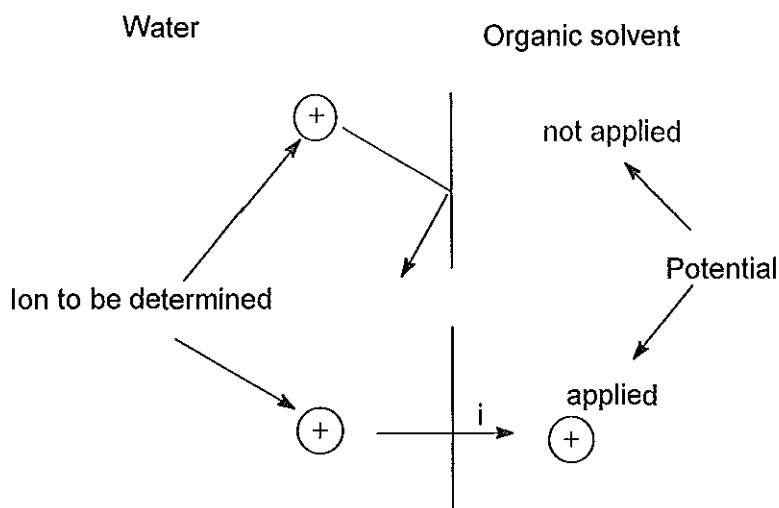


Figure 1 Transfer of ions across water/oil interface.

### 3.4. MATHEMATICAL TREATMENT OF CONCENTRATION PROFILE AT THE MEMBRANE STABILIZED IETIES

The theoretical solutions for the diffusion problem at the interface were obtained in order to get a clear picture about the diffusion of the substrate into the membrane of the sensor to be used. The analysis starts with the theoretical descriptions of the concentration profiles, which is a function of both time and distance from the electrode surface, and the response of the system to a current- step excitation in chronopotentiometric mode. Figure 2 below shows the supposed, normalized distance concentration profile prior to the application of a current-step ( $t \leq 0$ ) where O, M and W denote the space occupied by the organic, membrane and aqueous phase respectively.  $D_O, D_M$  and  $D_W$  are the diffusion coefficients in the respective phases. The membrane inserted has a thickness of  $a$ . The current,  $I$ , is acting at  $x=a$ . Semi-infinite diffusion is assumed in the aqueous phase and in the organic phase.



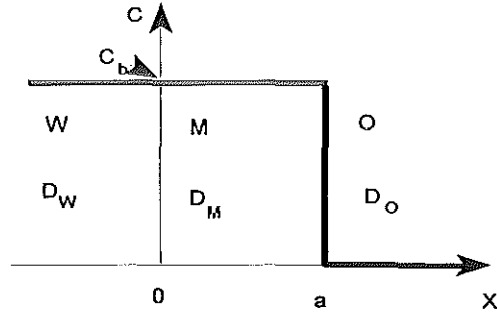


Figure 2. Distance concentration profile prior to application of a current step.

The calculation of the concentration profile  $C_O(x,t)$ ,  $C_M(x,t)$  and  $C_W(x,t)$  in the three regions requires the solution of linear diffusion equation.

$$\frac{\partial C_O(x,t)}{\partial t} = D_O \frac{\partial^2 C_O(x,t)}{\partial x^2} \quad (26)$$

$$\frac{\partial C_M(x,t)}{\partial t} = D_M \frac{\partial^2 C_M(x,t)}{\partial x^2} \quad (27)$$

and

$$\frac{\partial C_W(x,t)}{\partial t} = D_W \frac{\partial^2 C_W(x,t)}{\partial x^2} \quad (28)$$

Initial and boundary conditions

$$\text{At } t=0, \quad a < x < \infty; \quad C = C_O = 0 \quad (29)$$

$$-\infty < x < 0; \quad C = C_M = C_W = C_b \quad (30)$$

$$\text{For } t > 0 \quad C_O = 0; \quad X \rightarrow \infty \quad (31)$$

$$C_W = C_b; \quad X \rightarrow -\infty \quad (32)$$

$$C_W = C_M; \quad X = 0 \quad (33)$$

At  $x=a$ ;

$$D_M \frac{\partial C_M(x,t)}{\partial x} = \frac{i(t)}{nFA} \quad (34)$$

Flux balance is given by

At  $x=0$ ,

$$D_W \left( \frac{\partial C_W(x,t)}{\partial x} \right)_{x=0} = D_M \left( \frac{\partial C_M(x,t)}{\partial x} \right)_{x=0} \quad (35)$$

At  $x=a$

$$D_O \left( \frac{\partial C_M(x,t)}{\partial x} \right)_{x=a} = D_M \left( \frac{\partial C_M(x,t)}{\partial x} \right)_{x=a} \quad (36)$$

Laplace transform yields for the concentration profile in the three regions,

$$a < x < \infty; \quad C_O(x,s) = G(s) \exp[-q_O x] \quad (37)$$

$0 < x < a$ ;

$$C_M(x,s) = \frac{C_b}{s} + E(s) \exp[-q_M x] + F(s) \exp[q_M x] \quad (38)$$

and  $-\infty < x < 0$  ;

$$C_w(x,t) = \frac{C_b}{s} + B(s)\exp[q_w x] \quad (39)$$

Where

$$q_{(o,M,w)} = (s/D_{(o,M,w)})^{1/2} \quad (40)$$

The constants B(s), E(s), F(s) and G(s) have to be evaluated according to the boundary conditions and finally we obtain the concentration profile within the membrane in the Laplace domain

$$C_M(x,s) = \frac{C_b}{s} - \left( \frac{i(s)\Delta \exp[-q_M(x+a)]}{nFA s^{1/2} D_M^{1/2} (1+\sigma)(1+\Gamma \exp[-2q_M a])} + \frac{i(s)\Delta \exp[-q_M(3a-x)]}{nFA s^{1/2} D_M^{1/2} (1+\sigma)(1+\Gamma \exp[-2q_M a])} + \frac{i(s)\exp[-q_M(a-x)]}{nFA s^{1/2} D_M^{1/2}} \right) \quad (41)$$

Where  $\Gamma = (1-\sigma)/(1+\sigma)$  ,  $\sigma = (D_M/D_w)^{1/2}$  and  $\Delta = (1/D_w)^{1/2} - (1/D_M)^{1/2}$

The negative exponentials can be expanded in a series by the binomial theorem. Thus by letting  $i(s) = i/s$  for a current step applied ,equation 41 becomes:

$$C_M(x,s) = \frac{C_b}{s} - \frac{i}{nFA s^{3/2} D_M^{1/2}} \left( \frac{\Delta}{\Gamma} \sum_{n=0}^{\infty} (-1)^n \Gamma^n \exp[-q_M((2n+1)a+x)] + \frac{\Delta}{\Gamma} \sum_{n=0}^{\infty} (-1)^n \Gamma^n \exp[-q_M((2n+3)a-x)] + [\exp[-q_M(a-x)]] \right) \quad (42)$$

Where  $\eta=(1/D_M)^{1/2}+(1/D_M)^{1/2}$

From equation 42 the concentration profile in the time domain can be obtained by table transformation [52,53] and is :

$$\begin{aligned}
 C_M(x,t) = C_b - \frac{2it^{1/2}}{nFAD_M^{1/2}\pi^{1/2}} & \left( \left[ \frac{\Delta}{\eta} \sum_{n=0}^{\infty} (-1)^n \Gamma^n \exp - \frac{[(2n+1)a+x]^2}{4D_M t} \right] + \right. \\
 & \left. \left[ \frac{\Delta}{\eta} \sum_{n=0}^{\infty} (-1)^n \Gamma^n \exp - \frac{[(2n+3)a-x]^2}{4D_M t} \right] + \left[ \exp - \frac{[a-x]^2}{4D_M t} \right] \right) + \\
 & \frac{\Delta}{\eta} \sum_{n=0}^{\infty} (-1)^n \Gamma^n [(2n+1)a+x] \operatorname{erfc} \frac{[(2n+1)a+x]}{2(D_M t)^{1/2}} + (a-x) \operatorname{erfc} \frac{(a-x)}{2(D_M t)^{1/2}} \\
 + \frac{i}{nFAD_M} & \left( \frac{\Delta}{\eta} \sum_{n=0}^{\infty} (-1)^n \Gamma^n [(2n+3)a-x] \operatorname{erfc} \frac{[(2n+3)a-x]}{2(D_M t)^{1/2}} + \right.
 \end{aligned} \tag{43}$$

Since

$$\left( \frac{\partial C_M(x,t)}{\partial t} \right)_{x=a} = \text{constant}$$

at all times after onset of electrochemical process and  $C_M(a,t)$  can be obtained by setting  $x=a$  in equation 43 and is given by

$$C_M(a,t) = C_b - \frac{2it^{1/2}}{nFAD_M^{1/2}\pi^{1/2}} \left( 2 \frac{\Delta}{\eta} \sum_{n=0}^{n=\infty} (-1)^n \Gamma^n \exp \left[ \frac{-(n+1)^2 a^2}{D_M t} \right] + 1 \right) + \quad (44)$$

$$\frac{4ai}{nFAD_M} \left( \frac{\Delta}{\eta} \sum_{n=0}^{n=\infty} (-1)^n \Gamma^n (n+1) \operatorname{erfc} \left[ (n+1) \frac{a}{(D_M t)^{1/2}} \right] \right)$$

At certain characteristic time  $\tau$ , called the transition time,  $C_M(a,t)$  drops to zero. At this point equation 44 becomes

$$C_b = \frac{2t^{1/2}}{nFAD_M^{1/2}\pi^{1/2}} \left( 1 + 2 \frac{\Delta}{\eta} \sum_{n=0}^{n=\infty} (-1)^n \Gamma^n \exp \left[ \frac{-(n+1)^2 a^2}{D_M \tau} \right] \right) - \quad (45)$$

$$\frac{4ai\Delta}{nFAD_M\eta} \left( \sum_{n=0}^{n=\infty} (-1)^n \Gamma^n (n+1) \operatorname{erfc} \left( \frac{(n+1)a}{(D_M \tau)^{1/2}} \right) \right)$$

#### 4. EXPERIMENTAL

Different concentrations of  $\text{MgSO}_4$ (Analar) solutions were used as supporting electrolyte in the aqueous phase and 10mM Crystal violet tetraphenyl borate (CVTPB) or  $\mu$ -nitrido-bis(triphenylphosphorous)-3,3-como-bis-(undecahydro-1,2-cobaltaclosododecabor)ate (PNPDCC) in nitrobenzene in the organic phase. Nitrobenzene (Fluka) was purified by washing with 10% sulfuric acid and 10% sodium hydroxide and finally with distilled water until neutrality prior to use. This was used to prepare the organic phase. The aqueous solutions were prepared with double distilled water.

The electrochemical cell employed consisted of  $\text{Ag}/\text{AgCl}/\text{Cl}^-(\text{MgSO}_4)$  reference electrode immersed in different concentrations of  $\text{MgSO}_4$  aqueous solution and the second reference electrode also  $\text{Ag}/(\text{saturated KCl or } 0.1\text{M MgSO}_4 / \text{nitrobenzene (CVTPB) or (PNPDCC) interface. Dibenzo-18-crown-6 (Merck), NH}_4\text{Cl (BDH), CsCl (BDH), LiNO}_3 \text{ (Aldrich), LiClO}_4 \text{ (Ventron GmbH), Urea (Analar), NH}_4\text{NO}_3 \text{ ( Riedel-de-Haen) and urease (Mereck) were used as obtained commercially.}$

The electrochemical measurements were carried out with a four electrode potentiostat interface constructed in our laboratory connected to the electrochemical analyzer BAS100W (bioanalytical systems, Inc., USA). The IR drop was compensated manually to a point before the potentiostat starts oscillating. Different hydrophilic dialysis membranes and membrane filters were used to study their influence on the transfer of cations and anions. The membranes were swollen in water prior to mounting on the

amperometric sensor. The swollen membrane was mounted on teflon (PTFE) membrane holder, the inner compartment of which was filled with organic phase. The geometrical area of the interface was  $0.25\text{cm}^2$ .

For the study of the facilitated transfer of ions 20mM DB-18-C-6 was prepared in nitrobenzene containing the base electrolyte. The enzymatic sensor based on the membrane stabilized interface and the enzyme sandwiched between two dialysis membrane is shown in Figure 3a, and the amperometric sensor for urea consisting urease immobilized between dialysis membranes or millipore-filters (S&S) separating an organic electrolyte solution from the aqueous sample containing urea is shown in Fig 3b. Figure 4 and 5 show the block diagram of the experimental setups used in the experiments.

The electroanalytical techniques utilized for the investigation were dc-cyclic voltammetry, flow injection amperometry, differential pulse voltammetry, chronopotentiometry, chronoamperometry, chronocoulometry, and pulsed amperometry. All experiments were carried out at laboratory temperature ( $22 \pm 2^\circ\text{C}$ ).



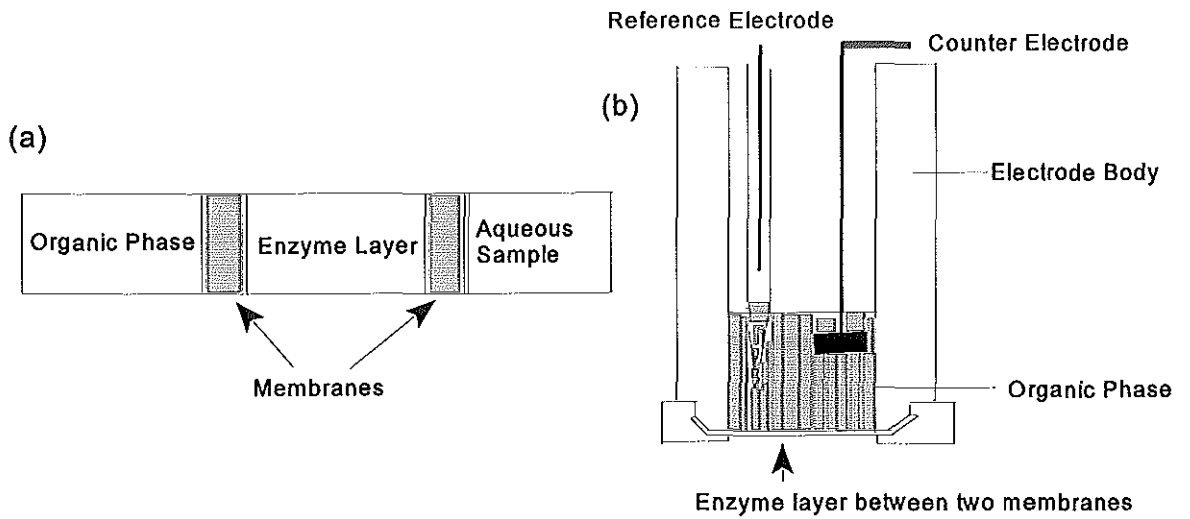


Figure 3. Membrane stabilized structure of the enzyme sensor (a), and amperometric sensor (b).

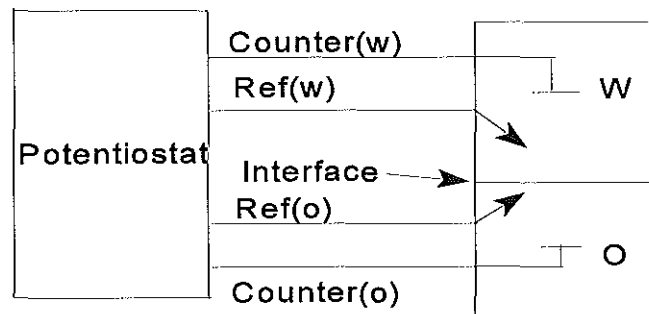


Figure 4. The four-electrode potentiostat.

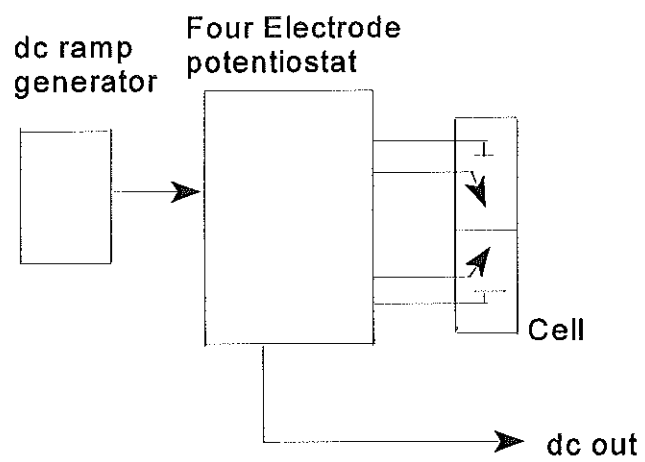


Figure 5. Block diagram of electronic setup for dc cyclic Voltammetry[54]

## 5. RESULTS AND DISCUSSION

### 5.1. THE INFLUENCE OF MEMBRANE ON SIMPLE ION TRANSFER

The ion transfer has been studied by cyclic voltammetry, flow injection amperometry, differential pulse voltammetry, chronoamperometry, chronocoulometry, chronopotentiometry and pulse amperometry. The membranes utilized were PT600, TP40, PT325, PT125, dialysis membrane from biology department. The thickness of the membrane were measured and the results are given in table 1. Results from IR spectra showed that all the membranes were cellulose acetate.

Table 1 The measured thickness of different membranes

Membrane type	Thickness(dry)/ $\mu\text{m}$	Thickness(swollen)/ $\mu\text{m}$
PT600		$73 \pm 2$
TP40		$40 \pm 2$
PT325	$20 \pm 1$	$41 \pm 1$
PT125	$10 \pm 2$	$20 \pm 2$

The ions chosen as a model were  $\text{Cs}^+$ ,  $\text{ClO}_4^-$  and  $\text{NO}_3^-$  for simple ion transfer and  $\text{NH}_4^+$  for facilitated transfer with DB-18-C-6 as a neutral carrier. The influence of supporting electrolyte concentration has been also investigated.

### 5.1.1. CYCLIC VOLTAMMETRY AT MEMBRANE STABILIZED INTERFACE

Figure 6a shows the cyclic voltammetry at membrane stabilized interface at different sweep rates. The peak to peak separation was 60mV which is expected for reversible diffusion controlled charge transfer reaction of univalent ion. At higher sweep rates, the diffusion layer thickness remains within the membrane so that it is possible to evaluate the diffusion coefficient for the ions within the membrane.

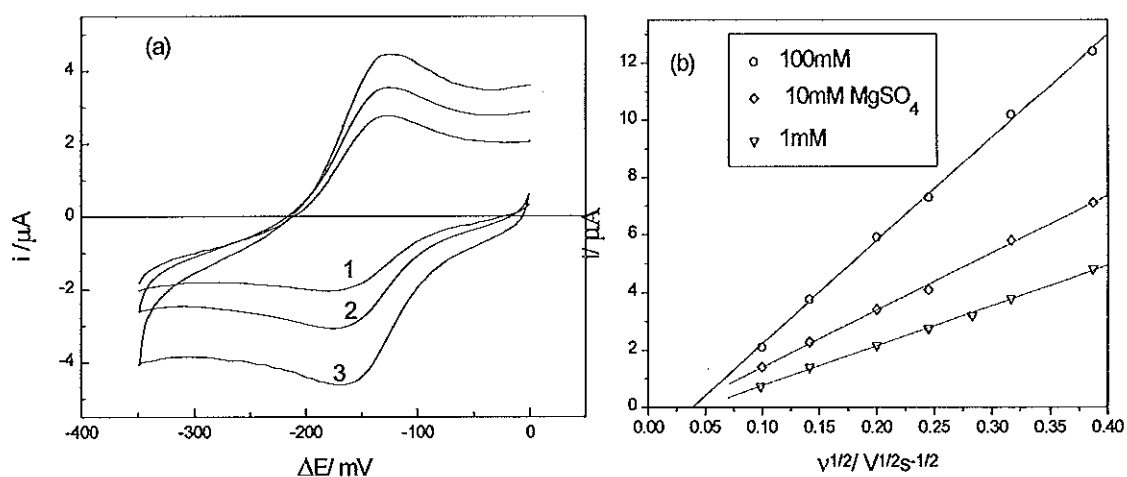


Figure 6(a). cyclic voltammogram and (b) The square root of sweep rate dependence on the peak current for the transfer of  $1\text{mM ClO}_4^-$  (water  $\rightarrow$  nitrobenzene). Sweep rates are 10,20 and 40mV/s for 1,2 and 3 respectively

Membrane: PT-600

It is interesting to see from Figure 6b that as the concentration of supporting electrolyte increased, there was an increase in the slope and the diffusion of  $\text{ClO}_4^-$ . The data extracted from Figure 6b is compiled in table 2.

Table 2 Diffusion coefficient of  $\text{ClO}_4^-$  evaluated from peak current versus the square root of sweep rate and from convoluted cyclic voltammogram.

C ( $\text{MgSO}_4$ ) / mM	Slope/ $\text{A s}^{1/2} \text{V}^{-1/2}$	$D_p/\text{Cm}^2\text{s}^{-1}$	$D_{\text{conv}}/\text{Cm}^2\text{s}^{-1}$	$i_{\text{conv}}/\text{A s}^{1/2}$
100	$5.2 \times 10^{-5}$	$6 \times 10^{-7}$	$3.6 \times 10^{-7}$	$1.45 \times 10^{-5}$
10	$4.2 \times 10^{-5}$	$3.9 \times 10^{-7}$	$2.5 \times 10^{-7}$	$1.2 \times 10^{-5}$
1	$2.3 \times 10^{-5}$	$1.2 \times 10^{-7}$	$4.3 \times 10^{-7}$	$5 \times 10^{-6}$

Since the voltammograms were not corrected for the base current the discrepancies were not so serious.

As it is evident from Figure 6a, the peak height is maximum in the limiting region. In this experiment the concentration of supporting electrolyte in the organic phase was 10mM CVTPB and the type of dialysis membrane employed was PT 600 regenerated cellulose acetate. The concentration of  $\text{LiClO}_4$  was 1mM. The series of experiments were carried out with different concentrations of  $\text{MgSO}_4$  as supporting electrolyte.

### 5.1.2. FLOW INJECTION AMPEROMETRY AT MEMBRANE STABILIZED INTERFACE

The transfer of  $\text{NO}_3^-$ ,  $\text{Cs}^+$  and  $\text{ClO}_4^-$  across membrane stabilized ITIES was investigated using flow injection amperometry. In this method, the axial concentration profile of the ion being investigated, which is caused by dispersion of the ion injected

sample plug in the laminar flowing carrier stream, the supporting electrolyte, is monitored by the current-time response.

When 100 $\mu$ L of standard solution of the ion under investigation was injected in to the carrier solution at different applied potentials within the polarization range of the supporting electrolytes, different current-time responses at different potentials were observed. By evaluating the peak heights of the current-time response, a curve which shows the dependence of the flow injection peak current on the applied potential difference was obtained (Figure 7). As it is obvious from Figure 7, the peak current is a maximum in the limiting current region.

The results of the investigation of ion transfer across membrane stabilized liquid/liquid interfaces indicate higher diffusion coefficients for cations over anions and in the case of anions gradual differences too. First results obtained with the membrane TP40 (Reichelt Chemietechnik) with nitrate, perchlorate and cesium ion are shown in Figure 8. For this experiment the supporting electrolyte in the organic phase ( nitrobenzene) was 10mM CVTPB and 5mM MgSO<sub>4</sub> was the carrier solution utilized. The sample injected (100 $\mu$ L) were not conditioned. Different flow rates were tried and best result was obtained at flow rate of 1mL/min and this was used in the experiment. The results of experiment are compiled in table 3.

Table 3: Results of flow injection amperometric experiment.

Ion	$i_l$ ( $\mu\text{A}$ )	$\Delta E_{1/2}$ (mV)	$\Delta\phi^0$ (mV) *	$\Delta E_{1/2,i} - \Delta E_{1/2}$ (mV)	$\Delta\phi^0_i - \Delta\phi^0$ (mV)	$r_{\text{crys}}$ ** (nm)	$r_{\text{hyd}}$ *** (nm)
$\text{NO}_3^-$	-3.80	9	-253	0	0	0.19	0.43
$\text{ClO}_4^-$	-2.06	192	-83	183	170	0.24	0.35
$\text{Cs}^+$	12.8	443	160	434	413	0.17	0.42

\* taken from ref [55],

\*\* taken from ref [57],

\*\*\* calculated from Stokes volume of hydrated ion.

The difference of the experimentally obtained half wave potentials between  $\text{NO}_3^-$  and  $\text{ClO}_4^-$  (183mV) and the difference between the standard Galvani potentials of the two ions (170mV) may be used to estimate the ratio of the apparent diffusion coefficients of the two ions within the aqueous side of the system. Based on

$$\Delta^w_o E_{\frac{1}{2}}^{(1)} - \Delta^w_o E_{\frac{1}{2}}^{(2)} = \Delta^w_o \phi^{0(1)} - \Delta^w_o \phi^{0(2)} + \frac{RT}{F} \ln \frac{Y_w^{(1)} Y_o^{(2)}}{Y_o^{(1)} Y_w^{(2)}} + \frac{RT}{2F} \ln \frac{D_o^{(1)} D_w^{(2)}}{D_w^{(1)} D_o^{(2)}} \quad (46)$$

and assuming that the activity coefficient term is very close to zero we obtain from experimental results

$$\left(\frac{D_{O}^{ClO_4^-} D_W^{NO_3^-}}{D_{O}^{NO_3^-} D_W^{ClO_4^-}}\right) = 10^{\left(\frac{0.013}{0.03}\right)} = 2.71$$

Estimating the diffusion coefficients in nitrobenzene by Stokes-Einstein relation [56] we obtain

$$\left(\frac{D_{ClO_4^-}}{D_{NO_3^-}}\right)_{org} = 0.79$$

i.e based on the crystallographic radii of  $ClO_4^-$  and  $NO_3^-$ . Therefore the ratio of the diffusion coefficient in the aqueous phase becomes

$$\left(\frac{D_{NO_3^-}}{D_{ClO_4^-}}\right)_W = \frac{2.71}{0.79} = 3.43$$

Since the limiting currents for the two ions under investigation depend on  $D^{1/2}$ ,  $i_l(NO_3^-)/i_l(ClO_4^-)$  is expected to be 1.85. The ratio of the experimentally obtained currents was 1.84. It is interesting to notice that the ratio of diffusion coefficient  $D(NO_3^-)/D(ClO_4^-)$  evaluated employing the ratio of their limiting current is in close agreement to the same ratio obtained employing Stokes-Einstein relation. Comparison of the limiting current of  $Cs^+$  with respect to  $NO_3^-$ , the ratio  $D(Cs^+)/D(NO_3^-) = (12.8/3.8)^2 = 11.35$ . This also



showed higher diffusion of  $\text{Cs}^+$  over  $\text{NO}_3^-$ .

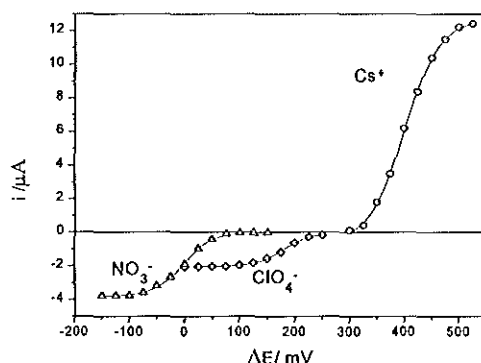


Figure 7 Dependence of peak current on the applied potential difference

Electrolytes: 10mM CVTPB in nitrobenzene and 5mM  $\text{MgSO}_4$  as a carrier

Experimental condition: Flow rate 1ml/min,  $C_{\text{ion}} 1\text{mmolL}^{-1}$

100 $\mu\text{L}$  of 1mM  $\text{CsCl}$ ,  $\text{LiNO}_3$  and  $\text{LiClO}_4$  injected.

### 5.1.3. DIFFERENTIAL PULSE VOLTAMMETRY OF MEMBRANE STABILIZED INTERFACE

For electroanalytical applications, differential pulse voltammetry is an interesting technique, as it provides sensitivity even better than those of normal pulse voltammetry and its detection limit is significantly lower ( $10^{-7}\text{M}$ ) due to more effective discrimination against the background (charging) current. This is because the current is sampled just before the pulse and at the end of the pulse and the difference in current is recorded as a function of the base potential.

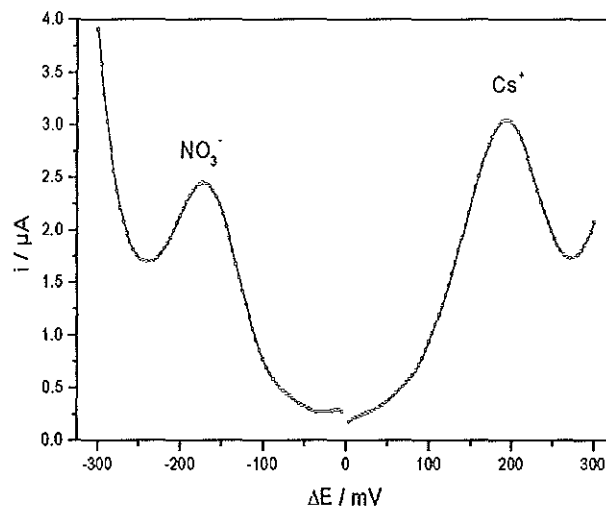


Figure 8. Differential pulse voltammetry of  $10^{-3}\text{M NO}_3^-$  and  $3 \times 10^{-4}\text{M Cs}^+$ .

Pulse width :1000ms, Pulse amplitude :20mV,  $i_p(\text{NO}_3^-)$  : $2.176 \times 10^{-6}\text{A}$  and

$i_p(\text{Cs}^+)$ : $2.75 \times 10^{-6}\text{A}$

Membrane: TP40

The result of differential pulse voltammetry shown in Figure 8 indicated that  $\text{Cs}^+$  diffuses faster than  $\text{NO}_3^-$ . In this experiment  $3 \times 10^{-4}\text{M CsCl}$  and  $10^{-3}\text{M LiNO}_3$  were used.

The diffusion coefficient within the membrane for  $\text{NO}_3^-$  was evaluated to be

$6.91 \times 10^{-7}\text{cm}^2/\text{s}$  and for  $\text{Cs}^+$   $1.226 \times 10^{-5}\text{cm}^2/\text{s}$  which means  $D(\text{Cs}^+) / D(\text{NO}_3^-) = 17.7$  or

$$\{D(\text{Cs}^+) / D(\text{NO}_3^-)\}^{1/2} = 4.21$$

#### 5.1.4 CHRONOAMPEROMETRY, CHRONOCOULOMETRY AND CHRONOPOTENTIOMETRY AT A MEMBRANE STABILIZED INTERFACE

In chronoamperometry (CA) and chronocoulometry (CC), the potential is stepped from one value to another, and the current (CA) or charge (CC) response is monitored as

a function of time. The initial potential is a potential at which no ion transfer occurs, and the final potential is the potential at which ion transfer occurs very rapidly. The current is therefore determined by the rate of mass transport from the bulk solution to the membrane stabilized interface, i.e., the rate of diffusion. The diffusion controlled Faradic current decays with  $t^{-1/2}$  (Cottrell equation). For diffusion controlled charge,  $Q$  is proportional to  $t^{1/2}$  (integrated form of Cottrell equation).

Chronocoulometry has an advantage over chronoamperometry. The signal increases with time, so the latter parts of the response, which are at least distorted by the finite charging time of the electrode, offer better signal-to-noise ratios. But for chronoamperometry the signal decreases with time.

The chronopotentiometric experiment was carried out by applying a controlled current between two counter electrodes, one on each side of the interface, and determining the response potential between two reference electrodes placed closely to each side of the interface. In a properly designed experiment the measured voltage reflects the voltage response of the interface.

Chronoamperometric and chronocoulometric modes were employed to investigate the influence of PT-325 membrane on the transfer of  $\text{NO}_3^-$  from water to nitrobenzene.

The results of chronoamperometry at different potential steps are compiled in table 4 from the current time response (Figure 9a). The slopes were related to Cottrell equation for planar electrode.

Table 4. Results of chronoamperometry at different potential steps for  $10^{-6} \text{ mol.cm}^{-3}$   $\text{LiNO}_3$ .

E/mV	Slope/ $\text{couls}^{-1/2}$	D/ $\text{cm}^2\text{s}^{-1}$
-250	$2.79 \times 10^{-5}$	$4.35 \times 10^{-6}$
-240	$2.74 \times 10^{-5}$	$4.16 \times 10^{-6}$
-230	$2.38 \times 10^{-5}$	$3.14 \times 10^{-6}$
-220	$2.14 \times 10^{-5}$	$2.55 \times 10^{-6}$
-200	$1.67 \times 10^{-5}$	$1.56 \times 10^{-6}$
-150	$6.48 \times 10^{-6}$	$2.34 \times 10^{-7}$
-100	$1.83 \times 10^{-6}$	$1.87 \times 10^{-7}$

Result of chronocoulometry at different potential steps are compiled in table 5. The data was extracted from the dependence of charge passed on the square root of time (Figure 10). The diffusion coefficients were evaluated by employing the integrated form of Cottrell equation.

Table 5. Results of chronocoulometry at different potential steps for  $10^{-6} \text{ molcm}^{-3}$   $\text{LiNO}_3$ .

E/mV	Slope/ $\text{couls}^{-1/2}$	D/ $\text{cm}^2\text{s}^{-1}$
-250	$5.54 \times 10^{-5}$	$4.26 \times 10^{-6}$
-240	$5.22 \times 10^{-5}$	$3.78 \times 10^{-6}$
-225	$4.26 \times 10^{-6}$	$2.9 \times 10^{-6}$

It can be seen from the values listed in table 5 that as the applied potential step becomes smaller negative the slope decreases. Especially for the applied potential more positive than -240mV , the slopes as well as the diffusion coefficients that are

evaluated using these slopes, are smaller compared to others. This is because they are not in the limiting current region. The results obtained from chronoamperometry are without correcting with respect to base current. If it has been done so a better result would have been expected.

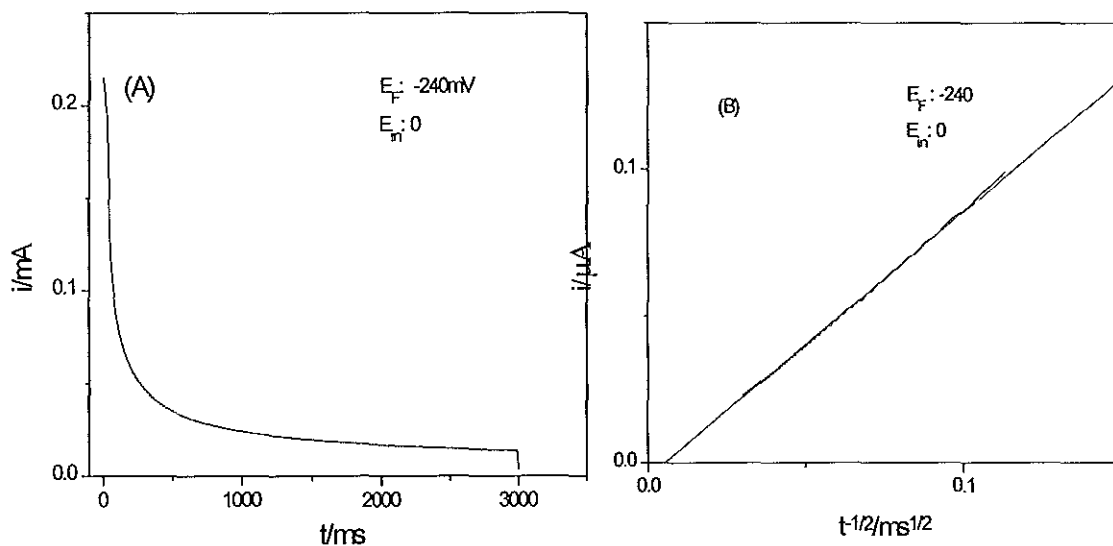


Figure 9 (A) Experimental chronoamperometric response of the membrane stabilized ITIES to a potential step excitation (current as a function of time) (B) current as a function of inverse square root of time. Membrane: PT325; Aqueous phase: 5mM  $\text{MgSO}_4$  + 1mM  $\text{LiNO}_3$ , Organic phase: 10 mM CVTPB in nitrobenzene.

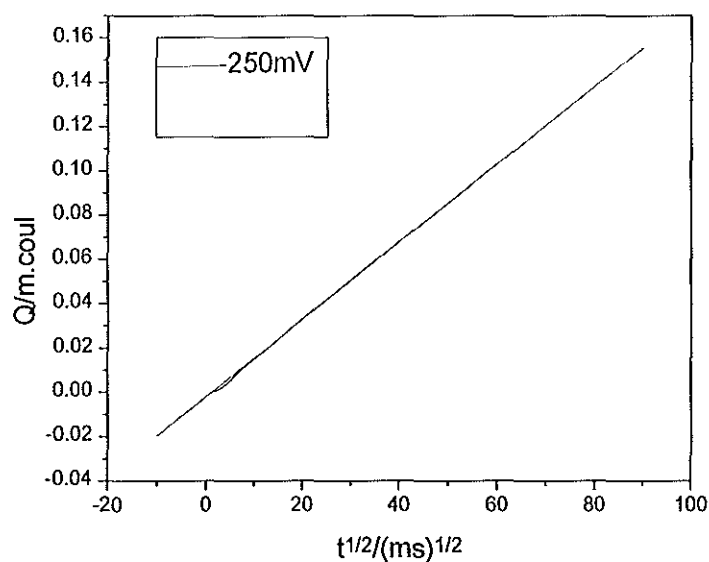


Figure 10. Experimental chronocoulometric response of the membrane stabilized ITIES to a potential step excitation.

The following figures show that experimentally obtained response of the membrane stabilized interface to a current step excitation in the chronopotentiometric modes. For potential step excitation in the chronoamperometric and chronocoulometric modes are shown in Figure 9(A) ,9(B) and Figure 10. As it is clearly seen, experimentally observed response characteristics are in accordance with those predicted by the theoretical expressions derived, and theoretical expressions derived in ref [58].

The results of experiments for PT-325 membrane employed to stabilized interface of chronopotentiometric mode at different concentrations of  $\text{LiClO}_4$  and different current steps applied are compiled in table 6 the data extracted from the plot of square root of transition time,  $\tau^{1/2}$ , as a function of inverse of current step applied,  $i^{-1}$  (Figure 12). The

expression for the slope is related to equation 44 for small  $t$  which reduces to Sand equation.

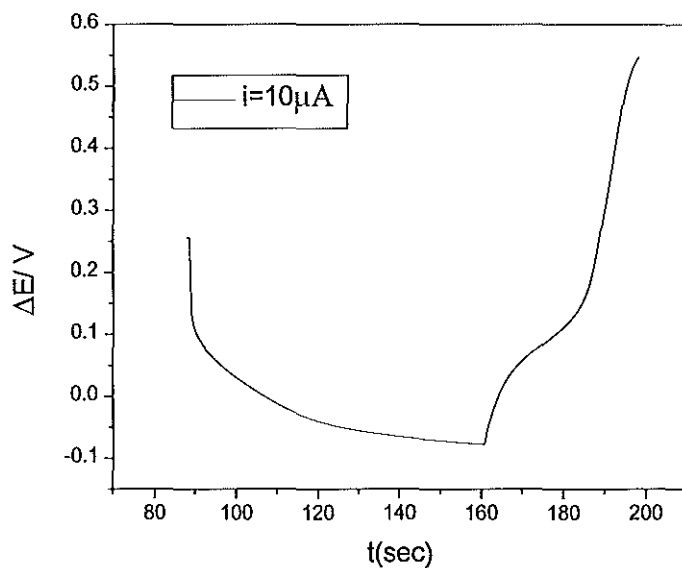


Figure 11. Experimental chronopotentiometric response of the membrane stabilized ITIES to a current step excitation.

Membrane: PT-125 , Aqueous phase: 5mM  $\text{MgSO}_4$  + 0.5mM  $\text{LiClO}_4$  ,

Organic phase: 10mM CVTPB in nitrobenzene

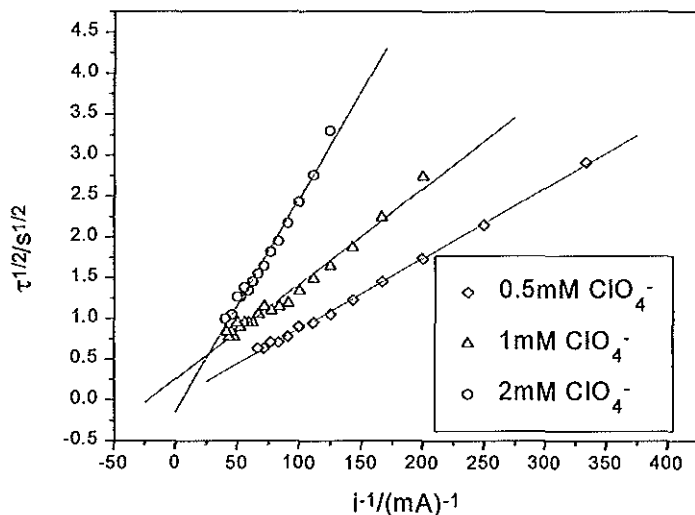


Figure 12. Inverse of current step dependence on the square root of transition time of the membrane stabilized ITIES.

Table 6. Data extracted from Figure 12

$C_{ClO_4^-} / \text{molcm}^{-3}$	Slope/ $\text{Coul.s}^{-1/2}$	$D / \text{cm}^2\text{s}^{-1}$
$5 \times 10^{-7}$	$8.62 \times 10^{-6}$	$6.7 \times 10^{-7}$
$10^{-6}$	$1.17 \times 10^{-5}$	$3.06 \times 10^{-7}$
$2 \times 10^{-6}$	$2.61 \times 10^{-5}$	$3.84 \times 10^{-7}$

When  $i\tau^{1/2}$ , the transition time constant is plotted against  $i$  Figure 13 is obtained.



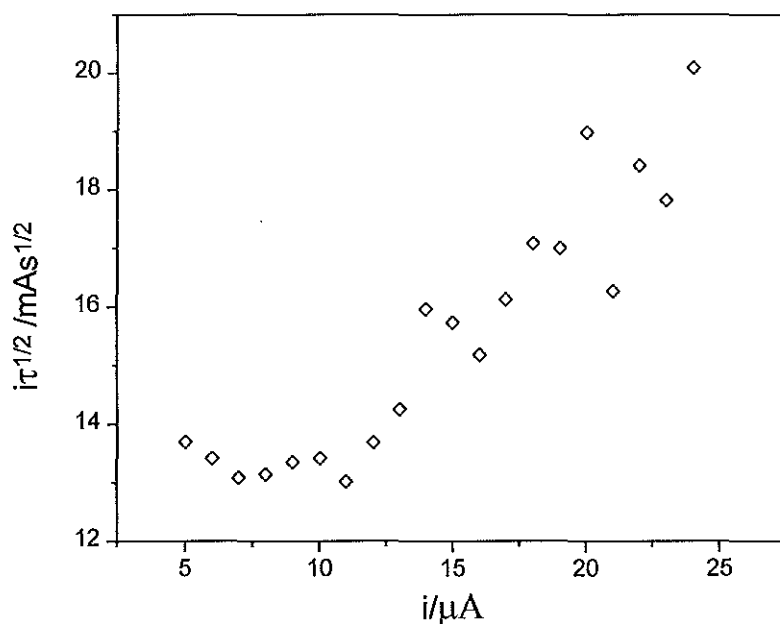


Figure 13 plot of transition time constant  $i\tau^{1/2}$  versus  $i$ .

It is clearly seen from Figure 12 and 13 that at extremely high and low current step there is a deviation from linearity. This is because at low current step the diffusion layer thickness grows out of the membrane since longer time is required for the ions to reach the interface. In contrast at extremely higher current step this time is shorter resulting in a large error in evaluating these small transition times.

## 5.2. THE CYCLIC AND DIFFERENTIAL PULSE VOLTAMMETRY STUDY OF THE FACILITATED TRANSFER OF AMMONIUM ION WITH DIBENZO-18-CROWN-6

The cyclic polyether dibenzo-18-crown-6, has six oxygen atoms in the polyether ring, that are the bond places of the ionophore, and two benzene rings as shown in figure 14. It forms a stable complex with ammonium ion by ion dipole interaction.

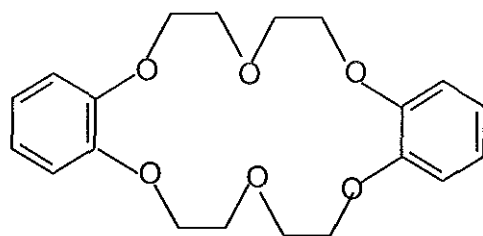


Figure 14. Dibenzo-18-crown-6.

In this study the organic phase was 10mM PNPDC as a supporting electrolyte solution and the transfer was facilitated by 20mM DB-18-C-6 with respect to the base electrolyte. The supporting electrolyte in the aqueous phase was 5mM  $\text{MgSO}_4$ .

The transfer of  $\text{NH}_4^+$  facilitated by DB-18-C-6 was studied using dc cyclic voltammetry (Fig 15.). The current peak height versus the square root of sweep rate (Fig 15a.) showed a linear dependence. This indicates the diffusion controlled transfer of the complex. Using the theory of linear potential sweep voltammetry at the stationary electrode [59], the diffusion coefficient  $D_{\text{NH}_4^+}$  in the membrane was evaluated to be  $2.3 \times 10^{-6} \text{cm}^2/\text{s}$ , from the peak currents corresponding to the transfer of  $\text{NH}_4^+$  from aqueous to nitrobenzene phase. The value of the diffusion coefficient in water,  $D_w$  which is  $1.96 \times 10^{-5} \text{cm}^2/\text{s}$  [60]. This is clearly due to the slow diffusion in side the membrane.

The transfer of  $\text{NO}_3^-$  was also studied in the same manner as  $\text{NH}_4^+$  and the diffusion coefficient in the membrane  $D_{\text{NO}_3^-}$  was evaluated to be  $1.48 \times 10^{-6} \text{cm}^2/\text{s}$ . Its diffusion coefficient in water is  $1.9 \times 10^{-5} \text{cm}^2/\text{s}$ . Results of investigation of facilitated ion transfer

across membrane stabilized liquid/liquid interface indicate higher diffusion coefficient for  $\text{NH}_4^+$  over  $\text{NO}_3^-$ . The result shows that both ions diffuse slower in the membrane compared to their diffusion in water.

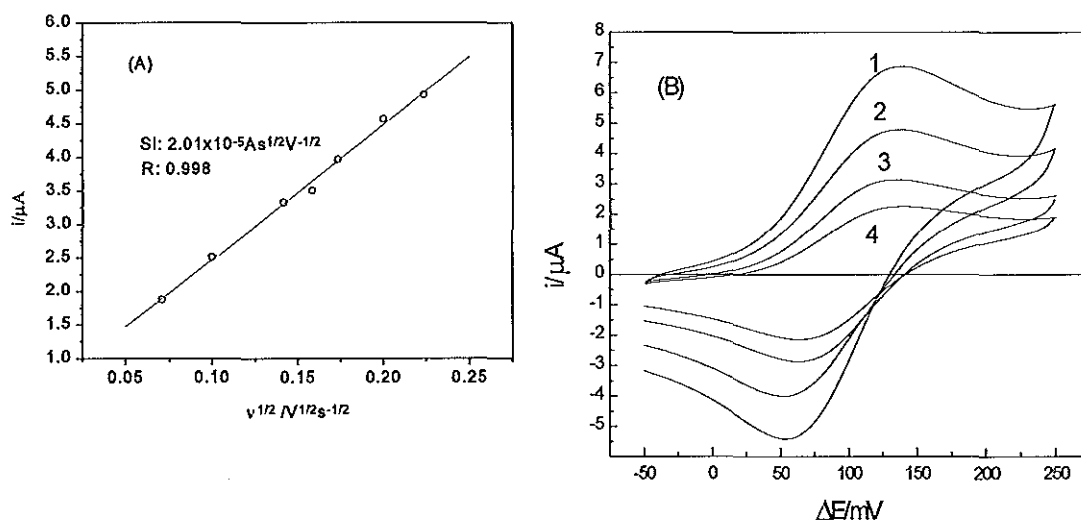


Figure 15 (A). Square root of sweep rate dependence on the peak current, and (B) cyclic voltammogram of  $2 \times 10^{-4} \text{M NH}_4^+$  at sweep rates of 50, 25, 10 and 5 mV/s for 1, 2, 3 and 4 respectively.

Differential pulse voltammetry experiment also showed faster diffusion of ammonium ion over nitrate.

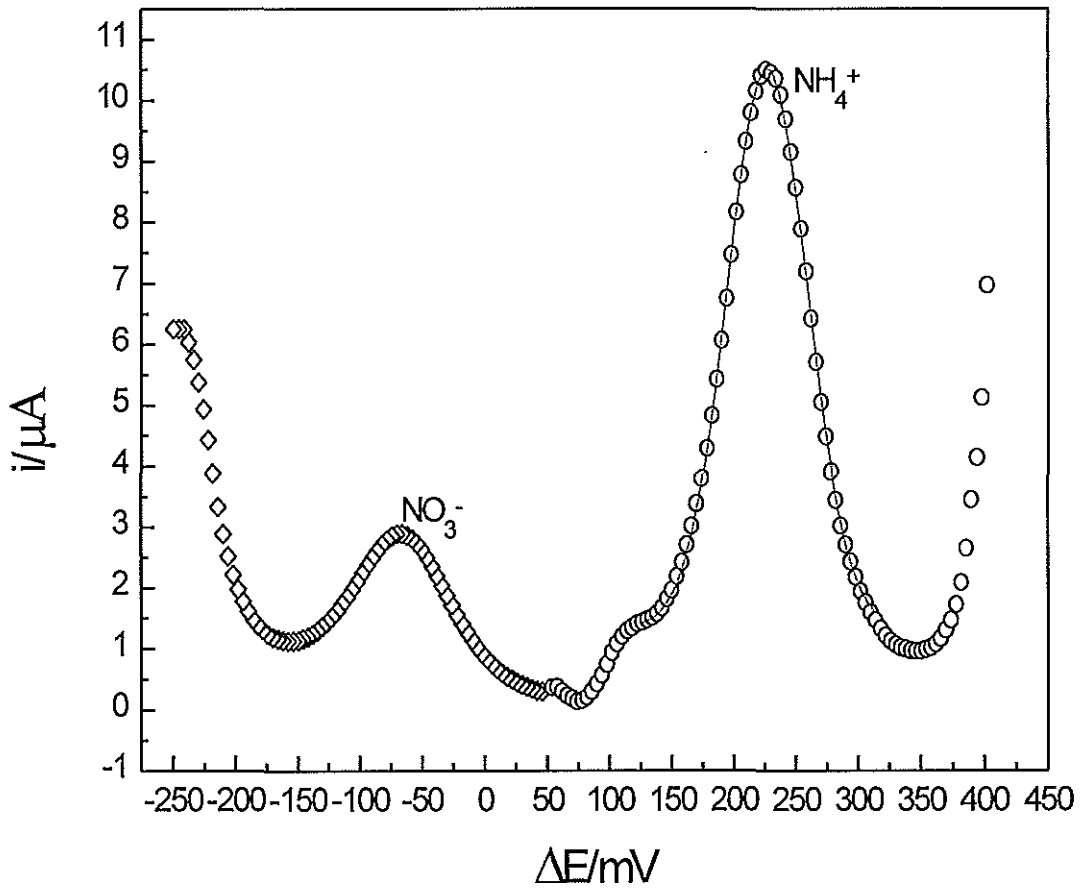
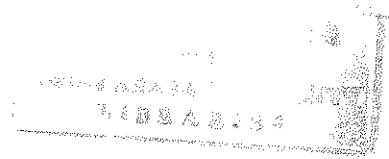


Figure 16. differential pulse voltammetry of  $2 \times 10^{-5}$  M  $\text{NH}_4\text{NO}_3$ .



### 5.3. THE INFLUENCE OF EMPLOYING SINGLE AND DOUBLE MEMBRANE ON THE FACILITATED TRANSFER OF AMMONIUM ION

The pulsed amperometric method, is also called the differential pulse time base (DPTB). Here, the potential excitation is done by a sequence of pulses of constant amplitude as shown in Figure 17. In DPTB, the current is sampled just before the pulse and at the end of the pulse so that there is effective discrimination against the background current. As it is the current difference that is displayed, the technique allows examination of defined potential window, which enhances the selectivity of the detection.

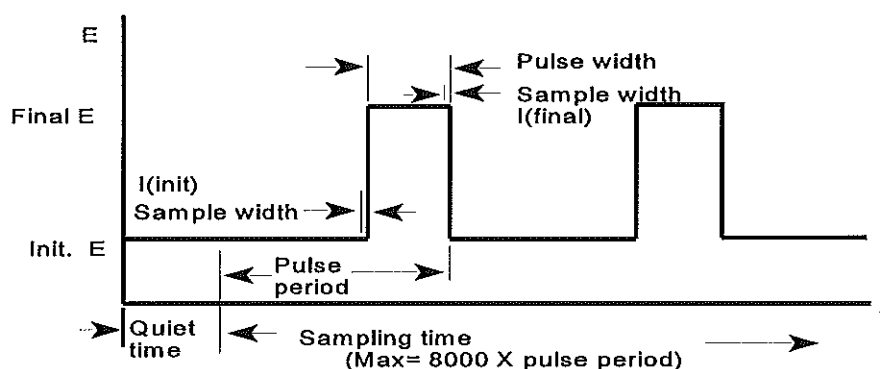


Figure 17. Potential excitation wave form for DPTB[61].

To see the influence of employing a single and double membrane on the transfer of ion under investigation a pulsed amperometric experiment was performed and the result is shown in Figure 18.

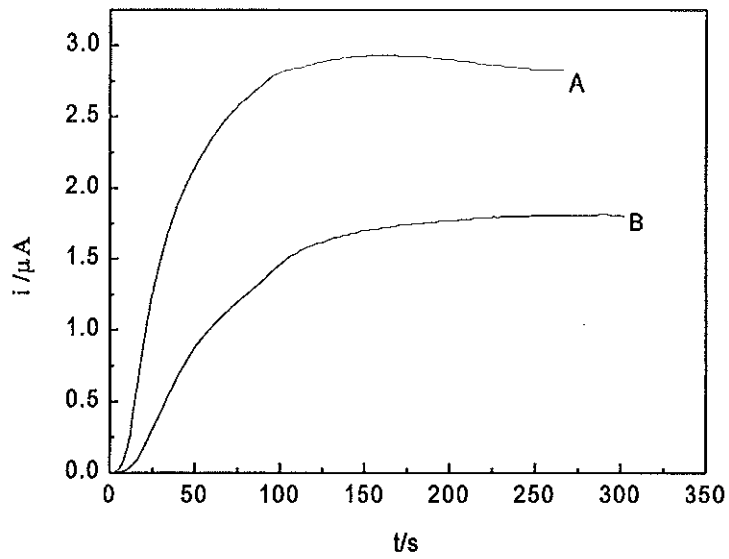


Figure 18. Pulsed amperometric sensor response to (A) single membrane and (B) double membrane.

The time constant ( $\tau$ ) ( the time needed for the current to reach 63% of its steady state value) for both cases was evaluated. This value was determined to be 39.8s and 70.69s for single and double membrane employed respectively. Similarly the steady state current was 2.93 $\mu$ A and 1.81 $\mu$ A. The decrease in current can be explained as follows.

Diffusion limited current at the membrane stabilized interface is given by:

$$i = nFAD_M \left( \frac{\partial C}{\partial x} \right)_{x=a,2a} \quad (47)$$

Where  $a$  is the thickness of the membrane. When the membrane thickness is doubled the current is halved and the time constant for double membrane employed was expected to be twice of the time constant for the single membrane. In this experiment the steady state current for the double membrane is slightly higher than half of the steady state current for the single membrane employed. This may be due to the non uniform thickness of the membrane.

The influence of gelatin layer on the transfer of  $\text{NH}_4^+$  is shown in Figure 19. As can be seen from the graph the sensitivity is low compared to single or double membrane employed and it needs longer time to reach steady state current.

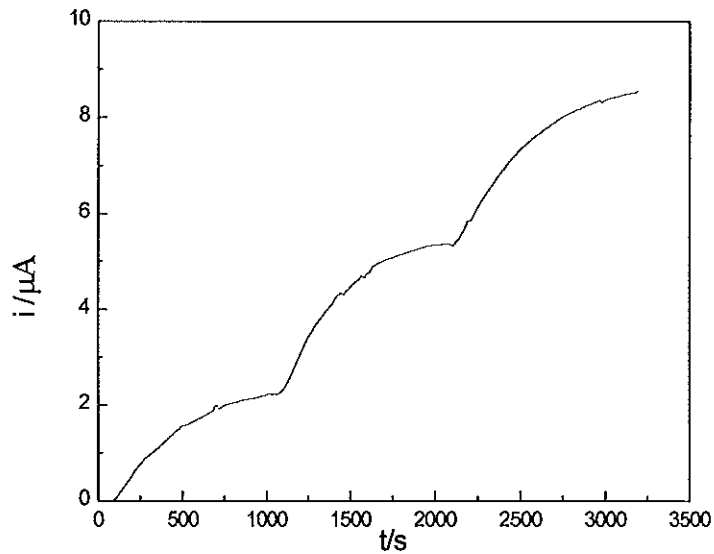


Figure 19. Pulse amperometric response after incorporating gelatin between two membranes.

#### 5.4. THE RESPONSE BEHAVIOR OF THE UREA SENSOR

The quantitative determination of ammonium ion can be performed by different electroanalytical techniques and is based on the proportionality of the current due to the facilitated transfer to concentration. Figure 20(A) shows the cyclic voltammogram for different concentration of ammonium ion and Figure 20(B) shows the concentration dependence of peak current of cyclic voltammogram at a sweep rate of 25mV/s. Pulse amperometric measurement was easier for the evaluation of results. One requirement for this type of measurement is to keep the thickness of the diffusion layer constant. This can be achieved by stirring the analyte. Constant stirring generates a series of steps. The working potentials for pulsed amperometry were chosen to come as close as possible to values corresponding to the limiting current range of the investigated ion transfer.

Pulsed amperometry has advantage of higher sensitivity and the ions which were transferred at positive potentials were transferred back to the aqueous phase at the second potential chosen sufficiently negative. The sensitivity of the method depends on the potentials chosen and cannot be considered as a constant. However the calibration experiments have shown that the method is suitable for the determination of ammonium ion.



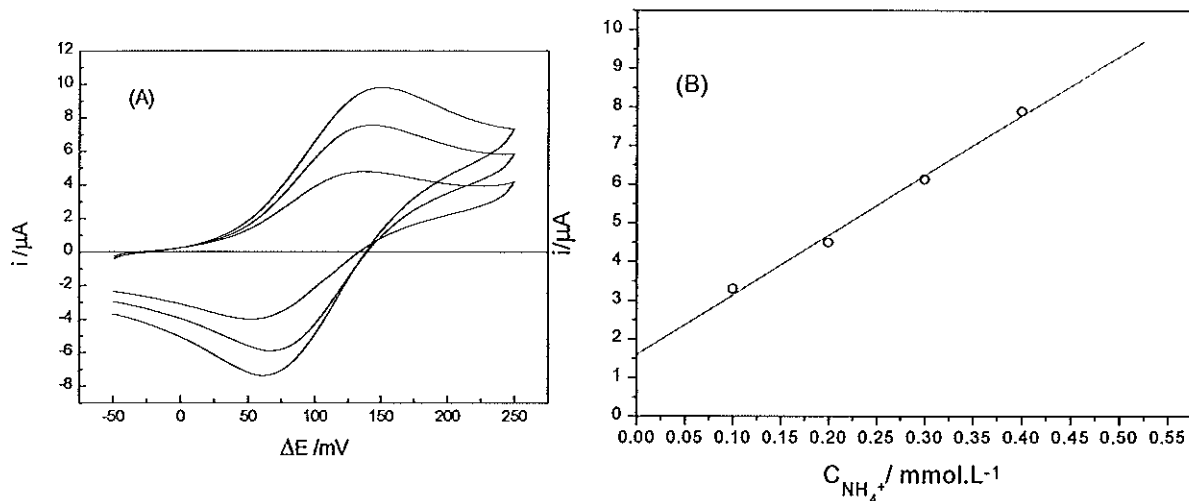


Figure 20(A) Cyclic voltammograms of the membrane stabilized water/nitrobenzene interface at increasing concentration of  $\text{NH}_4^+$ . The concentration change between cycles is  $2 \times 10^{-5} \text{ mol/L}$ . (B) Concentration dependence on peak current at sweep rate of  $25 \text{ mV/s}$ .

The quantitative determination of ammonium ion is shown in Figure 21a and b. As one can see from the graph the limiting current is directly proportional to the concentration of ammonium ion present. The concentration of DB-18-C-6 in the nitrobenzene was  $20 \text{ mM}$  which is greater than the concentration of ammonium ion in the aqueous phase. This indicates that the limiting current is controlled by diffusion of this ion from bulk of the aqueous phase to the membrane stabilized interface.

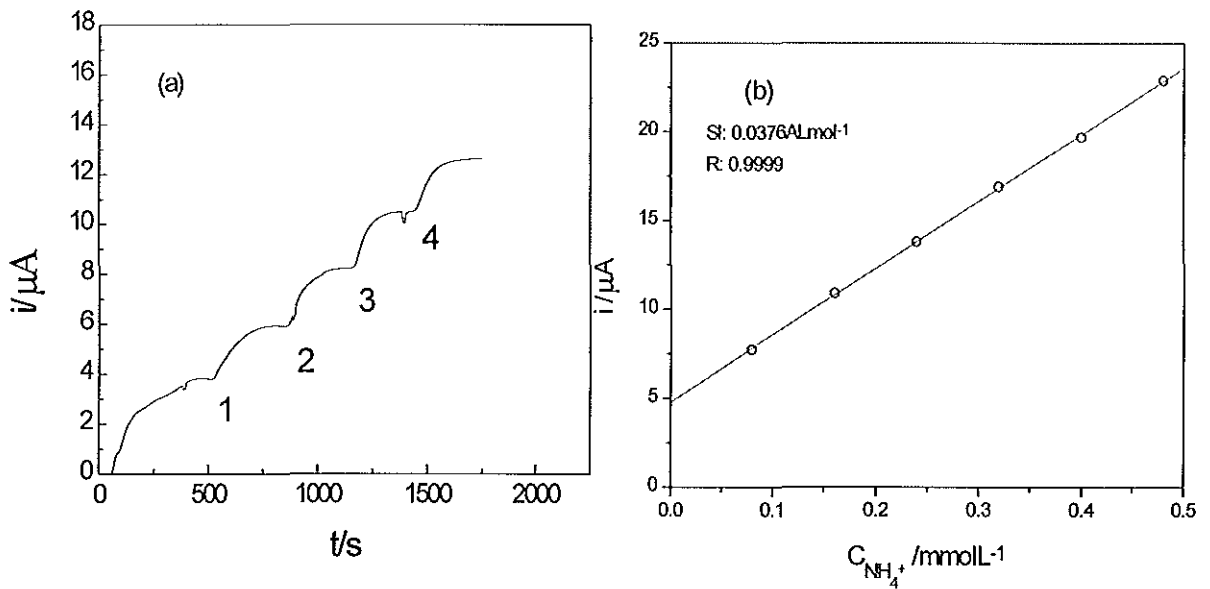


Figure 21(a) Pulse amperometric sensor response to concentration steps of  $0.02\text{mM}$   $\text{NH}_4^+$ , (b) Calibration curve for  $\text{NH}_4^+$  ion obtained by pulsed amperometry.

$$E_{\text{in}} = -200\text{mV}, E_{\text{fn}} = 150\text{mV}.$$

For the quantitative determination of urea, an amperometric sensor ( Figure 3), with immobilized urease enzyme was employed. When urea enters into the enzyme layer in the sensor, it will be converted into ammonium ion by urease. When a potential is applied the facilitated transfer of  $\text{NH}_4^+$  occurs which in turn is proportional to the concentration of urea.

Calibration of the sensor was made by adding standard solutions of ( $0.1\text{M}$  of  $40\mu\text{L}$  or  $80\mu\text{L}$ ) of urea to a  $50\text{mL}$  of  $5\text{mM}$   $\text{MgSO}_4$  solution used as supporting electrolyte and was carried out by measuring the steady-state response of the sensor by pulse amperometry.

The ammonium ion is released from the urease action on urea present in the amperometric sensor according to the reaction:



The calibration curve for quantitative determination of urea is shown in figure 22a and b. As can be seen from the graph the limiting current is directly proportional to the concentration of urea present. In this experiment the time constant was determined to be 250 sec.

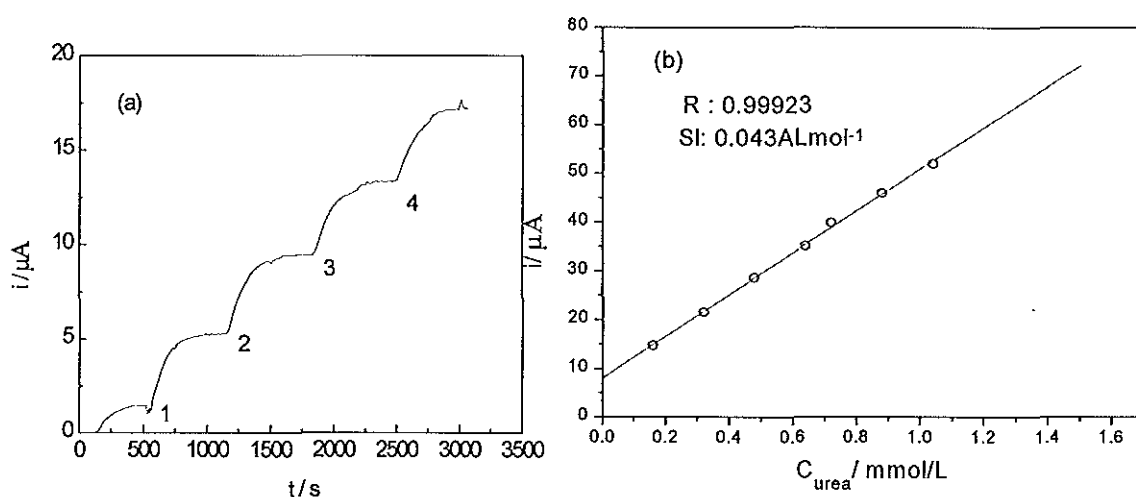


Figure 22(a) Pulse amperometric response to concentration steps of 0.08mM, 1; 0.16mM 2, 3 and 4 of urea respectively.

As the pulse amperometric experiment shows, the response time for the sensor is so long that it can not be applicable for the determination of urea. Further investigation of membrane material which is applicable for this purpose is needed.

## 6. CONCLUSIONS

Different electrochemical methods were made in this work. The influence of the membrane materials employed in the simple and facilitated ion transfer of  $\text{Cs}^+$ ,  $\text{NH}_4^+$ ,  $\text{ClO}_4^-$  and  $\text{NO}_3^-$  was studied. According to this study the diffusion coefficients of these ions was found to be ten or hundred times smaller than their diffusion coefficient in water. The results of this investigation indicate higher diffusion coefficients for cations over anions and in the case of anions gradual differences too.

A theoretical model has been developed for the response behavior and theoretical equations has been derived for current step excitation. The experimental results were in agreement with the theoretical equations.

Calibration of the amperometric sensor for ammonium ion was performed employing pulse amperometric mode. The applicability of the amperometric sensor with immobilized urease enzyme for the determination of urea has been studied employing DB-18-C-6 as a neutral carrier in the organic phase. The ammonium ion generated by enzymatic action on the urea was sensed by the sensor. The response time for the sensor was found to be very long. Further investigation of the membrane materials is required for the applicability of the sensor.

18. A.G. Volkov, M.I. Gugoshashvili, A.F.Mironov and L.I. Bogulavousky, *Bioelectrochem.Bioenergy*, 9(1982)551.
19. A.G. Volkov, M.I. Gugoshashvili, A.F.Mironov and L.I. Bogulavousky, *Bioelectrochem.Bioenergy*, 10(1983)485.
20. W.J. Albery, A.M. Couper, J. Hadgreff and C. Ryan, *J. Chem. Soc., Faraday Trans.1*,70(1974)1124.
21. W.J. Albery, R.A. Choudhery and P.R. Fisk, *Faraday. Discuss.Chem.Soc.*, 77(1984)53.
22. B. Hundhammer, S.K.Dhawan, A.Bekele and H.J. Seidlitz, *J. Electroanal. Chem.*,217(1987)253.
23. J. Koryta, *Electrochim. Acta*, 24(1979)293.
24. A.Hofmanova,L.Q.Hung and W. Khalil, *J. Electroanal. Chem.*,135(1982)257.
25. Z.Samec, D. Homolka, and V.Marecek, Khalil, *J. Electroanal. Chem.*,135(1982)265.
26. D. Homolka, K.Holub, and V.Marecek, *J. Electroanal. Chem.*,138(1982)29.
27. E.Makrlik, L.Q. Hung, and A. Hofmanova, *Electrochem. Acta.*,28(1983)847.
28. P. Vanysek, W. Ruth, and J, Koryta, *J. Electroanal. Chem*,148(1983)117.
29. E.Makrlik, L.Q Hung, Koryta, *J. Electroanal. Chem*,158(1983)117.
30. E.Makrlik, *J. Colloid Interface. Sci.*,97(1984)595.
31. J, Koryta, G.Du, W.Ruth and Vanysek, *Faraday Discuss.Chem.Soc.*,77(1984)209.
32. W.Erkang and P.Zhicheng, *J.Electroanal.Chem.*,189(1985)21.
33. Z.Yoshida and H. Freiser, *J. Electroanal. Chem.*, 179(1984)31.
34. J, Koryta, *Ion-Selective Electrode Rev.*, 5(1983)146.
35. L. Sinru and H,Freiser, *J. Electroanal. Chem.*, 191(1985)437.

36. T. Kakutani, Y. Nishiwaki, T. Osakai, and M. Senda, *Bull. Chem. Soc. Jpn.*, **59**(1986)781.
37. J. Koryta and P. Vanysek in H. Gerischer and C.W. Tobias (Eds), *Advances in Electrochemistry and Electrochemical Engineering*, Vol 12, Wiley-Interscience, New York, **1981**, PP.113.
38. J. Koryta, *Electrochim. Acta* **29**(1984)445.
39. P. Vanysek and R.P. Buck, *J. Electroanal. Chem.*, **163**(1984)1.
40. B. Hundhammer, T. Solomon and B. Alemayehu, *J. Electroanal. Chem.*, **135**(1982)301.
41. P. Vanysek, *J. Electroanal. Chem.*, **121**(1981)149.
42. B. Hundhammer, T. Solomon and B. Alemayehu, *J. Electroanal. Chem.*, **149**(1983)179.
43. A.J. Bard, *Electroanalytical Chemistry*, Vol. 15, Marcel Dekker Inc., New York, **1989**.
44. Z. Samec, V. Měrecký and J. Weber, *J. Electroanal. Chem.*, **100**(1979)841.
45. D. Britz, *J. Electroanal. Chem.*, **88**(1978)309.
46. J. Parker, *J. Chem. Rev.*, **69**(1969),1.
47. C. Gavach, F. Henery, *J. Electroanal. Chem.*, **54**(1974)361.
48. J. Koryta, P. Vanysek, M. Brezina, *J. Electroanal. Chem.*, **75**(1975)211.
49. R. Parsons, *The Structure of the Electrical Double Layer and its influence on the rates of Electrode Reactions*, in *Advances of Electrochemistry and Electrical Engineering*, Vol 1, Delahay, P. Ed; Interscience, New York, **1961**, Chapter 1.
50. D. Homolka, L. Q. Hung, A. Hofmanova, M. Khalil, J. Koryta, V. Měrecký, Z. Samec, S.K. Sen, J. Weber and M. Brezina, *Anal. Chem.*, **52**(1980)1606.
51. S. Wilke, H. Franzke and H. Müller, *Anal. Chim. Acta.*, **268**(1992)285.